1-1-2016

A Computationally Efficient Method for Calculation of Strand Eddy Current Losses in Electric Machines

Alireza Fatemi
Marquette University

Dan M. Ionel
University of Wisconsin - Milwaukee

Nabeel Demerdash
Marquette University, nabeel.demerdash@marquette.edu

Dave A. Staton
Motor Design, Ltd.

Rafal Wrobel
Motor Design, Ltd.

See next page for additional authors

Accepted version. *2016 IEEE Energy Conversion Congress and Exposition* (2016). DOI.

A Computationally Efficient Method For Calculation Of Strand Eddy Current Losses In Electric Machines

Alireza Fatemi
Department of Electrical and Computer Engineering, Marquette University, Milwaukee, WI
Dan M. Ionel
Department of Electrical and Computer Engineering, University of Kentucky, Lexington, KY
Nabeel A. O. Demerdash
Department of Electrical and Computer Engineering, Marquette University, Milwaukee, WI
Dave A. Staton
Motor Design Ltd., Ellesmere, UK
Rafal Wrobel
Motor Design Ltd., Ellesmere, UK
Yew Chuan Chong
Motor Design Ltd., Ellesmere, UK

Abstract: In this paper, a fast finite element (FE)-based method for the calculation of eddy current losses in the stator windings of randomly wound electric machines with a focus on fractional slot concentrated winding

2016 IEEE Energy Conversion Congress and Exposition (ECCE), (2016). DOI.

(FSCW) permanent magnet (PM) machines will be presented. The method is particularly suitable for implementation in large-scale design optimization algorithms where a qualitative characterization of such losses at higher speeds is most beneficial for identification of the design solutions which exhibit the lowest overall losses including the ac losses in the stator windings. Unlike the common practice of assuming a constant slot fill factor, sf, for all the design variations, the maximum sf in the developed method is determined based on the individual slot structure/dimensions and strand wire specifications. Furthermore, in lieu of detailed modeling of the conductor strands in the initial FE model, which significantly adds to the complexity of the problem, an alternative rectangular coil modeling subject to a subsequent flux mapping technique for determination of the impinging flux on each individual strand is pursued. The research focus of the paper is placed on development of a computationally efficient technique for the ac winding loss derivation applicable in design-optimization, where both the electromagnetic and thermal machine behavior are accounted for. The analysis is supplemented with an investigation on the influence of the electrical loading on ac winging loss effects for a particular machine design, a subject which has received less attention in the literature. Experimental ac loss measurements on a 12-slot 10-pole stator assembly will be discussed to verify the existing trends in the simulation results.

SECTION I.

Introduction

The eddy current effects including the skin, strand-level, and bundle-level proximity effects[1] potentially constitute a significant contributor to the overall copper losses in the stator windings of high speed permanent magnet (PM) machines. Even if preventive measures such as stranding and transposition are adopted, the ac conductor losses in the stator windings of PM motors can still be significant for high power density-high speed open-slot fractional-slot concentrated winding (FSCW) machines due to the prevalence of slot leakage flux, and slot opening fringing flux, e.g. see Fig. 1. Common techniques for the estimation of such losses are especially prohibitive for randomly wound coil configurations and require a significant amount of time to formulate and solve the ac electromagnetic problem at the conductor strand level. The development of a high-fidelity loss characterization method to provide a basis of qualitative ac loss comparison between thousands of design candidates, which is suitable for implementation in large-scale design optimization algorithms, is imperative. In addition to the value of the ac loss, the distribution of the overall copper losses in the stator winding is of interest particularly if coupled-thermal electromagnetic design optimization is desired.[2,3]

In a broad categorization, the popular methods for analysis of eddy current losses in PM machines rely on analytical models as in,[4–5,6,7,8,9,10,11,12] numerical finite element/difference analysis as in,[13–14,15,16] or rely on combined analytical-FE-experimental procedures as in.[17–18,19] The analytical models lack the desired accuracy under magnetic core saturation and are not applicable to complex geometry without compromising further the accuracy. The numerical models are not suitable for integration into large-scale design optimization processes due to time consuming computations. The combined procedures require extensive a priori experimentations

2016 IEEE Energy Conversion Congress and Exposition (ECCE), (2016). DOI.

and are best suited for accurate loss analysis between different motor and winding configurations as opposed to application for large-scale design optimization of one particular configuration.

In this paper, a finite element (FE)-based modeling technique is presented for estimation of the strand eddy current losses in the stator windings of electric machines, with an emphasis on sinusoidally excited PM synchronous machines. This is in order to include the portion of the ac losses which stems from the presence of slot leakage and fringing fluxes in the performance characterization of such machines. The developed hybrid analytical-numerical loss calculation method is rendered computationally efficient through adopting several measures such as alternative coil modeling which reduces the computation time required for solving the FE model, exploiting the existing electric symmetry in addition to the magnetic periodicity of PM machines with sinusoidal current excitation, and implementing fast analytical techniques for mapping the flux within the slot area, estimating the fill factor and strand locations, and finally characterization of the eddy current losses based on the value of the flux density impinging on each stator winding conductor. The presented loss calculation method provides a reasonable compromise between computational time and accuracy, which makes it suitable for application in large-scale design optimization of PM machines in the initial stages of the design.

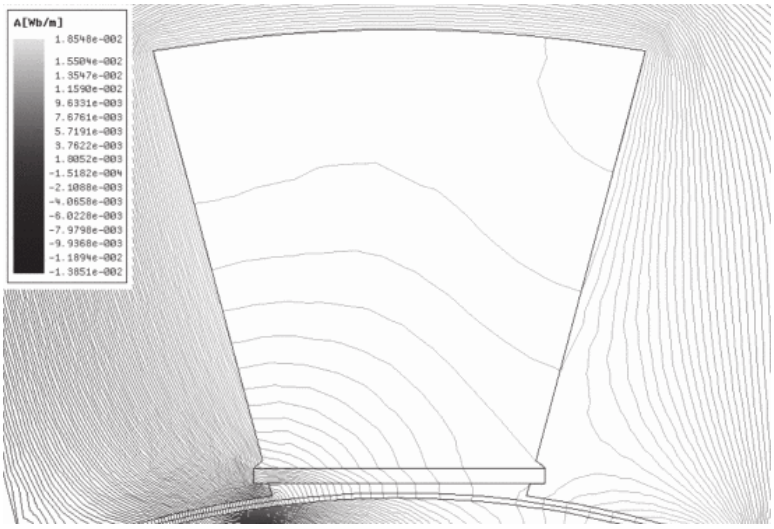

Fig. 1. Slot leakage and fringing flux in a typical FSCW PM machine.

Using the developed method, strand eddy current losses under various loading conditions are computed and the existing trends between the ratio of ac to dc losses, P_{ac}/P_{dc}, with respect to the loading level are studied. Through this analysis, it is demonstrated that the traditional figure of merit for comparison of ac losses in electric machines, which is established by the ratio of ac to dc resistance, R_{ac}/R_{dc}, is by definition incapable of modeling the effects of the loading level on the ratio of P_{ac}/P_{dc}.

SECTION II.

Strand Eddy Current Loss Characterization

Analytical models are reported for (a) 1-D single-slot models as in,[8] (b) 2-D single-slot models as in,[9] or (c) 2-D machine models as in.[10] These methods provide an insight into the nature of eddy current losses but do not accurately account for the non-linearity of the magnetic core, and are difficult to apply to complex machine geometries.

Numerical models require a significantly large number of elements in the stator slots and are therefore time-consuming. In some studies with detailed coil models,[13,15] a uniform distribution of current is assumed in the conductors so that a time-stepping magnetostatic solution can be performed. Subsequently, a detailed distribution of the radial and tangential components of flux density, $B_{R,T}$, in each stator slot is obtained by establishing a fine grid over each slot pitch of the stator from one tooth axis to the next. These values are used in a numerical harmonic analysis expressed by:

$$B_{R,T}(t) = \sum_{k=1}^{\infty} |B_{2k-1,(R,T)}| \sin((2k-1)\omega t - \phi_{2k-1,(R,T)}) \quad (1)$$

Accordingly, the eddy current loss, P_e, in watts per strand per depth of axial length, for a rectangular copper strand of width a, and height b subject to a uniform time varying flux density of (1) can be obtained using:

$$P_e = ab \sum_{k=1}^{\infty} \frac{(2k-1)^2\omega^2}{24\rho} (|B_{2k-1,R}|^2 a^2 + |B_{2k-1,T}|^2 b^2) \times \eta_{2k-1} \quad (2)$$

where the skin effect coefficient η_{2k-1} is given by:[20]

$$\eta_{2k-1} = \frac{3}{4\alpha_{2k-1}^2} \quad \frac{\sinh(2\alpha_{2k-1}) - \sin(2\alpha_{2k-1})}{\cosh(2\alpha_{2k-1}) - \cos(2\alpha_{2k-1})},$$
$$\alpha_{2k-1} = \frac{a}{6320}\sqrt{\frac{\mu_r(2k-1)f}{\rho}}$$

(3)

In the case of round conductors of diameter d, and resistivity ρ, (1) can be used for calculating the magnitude of the impinging flux $|B_{2k-1}| = \sqrt{|B_{2k-1,R}|^2 + |B_{2k-1,T}|^2}$, with the eddy current loss per depth of axial length given by:[1]

$$P_e = \pi d^4 \sum_{k=1}^{\infty} \frac{(2k-1)\omega^2 |B_{2k-1}|^2}{128\rho}$$

(4)

The ratio of ac to dc resistance, r_{ac}, of round conductors can be modified according to (5) in order to also include the skin effect:[1]

$$r_{ac} = \frac{d}{8\delta} Re((1+j)\frac{I_0(\frac{d}{2\delta}(1+j))}{I_1(\frac{d}{2\delta}(1\{j))}), \delta = \sqrt{\frac{2\rho}{\omega\mu}}$$

(5)

where I_0 and I_1 are Bessel functions of zero and first orders, respectively, and δ is the skin depth. The solution of r_{ac} for round conductors is documented through charts and graphs in,[1] and can be readily found for a given conductor diameter and excitation frequency.

SECTION III.

Fe-Based Eddy Current Loss Estimation for Randomly Wound Stator Windings

2016 IEEE Energy Conversion Congress and Exposition (ECCE), (2016). DOI.

For a given machine configuration, the distribution of the leakage/fringing flux within any slot is dependent on:

- various dimensions of the cross section,
- the loading level,
- the location of the conductors within the stator slots,
- the temperatures of various components, and
- the frequency of operation.

Only a thermally coupled-time-harmonic finite element (FE) model with detailed knowledge of conductor locations can account for all the aforementioned parameters. The formulation and solution of such an electromagnetic (EM) problem is an extensively and computationally demanding process, not suitable for early design stage optimization purposes.

In this section, an alternative method will be presented. The steps of this computationally efficient loss calculation method which can be integrated into a large-scale design optimization process are described in the following section.

A. Modeling of the Coils

Detailed modeling of the coils in the slots, such as the one shown in Fig. 2(a), adds to the complexity of the FE model, and thus increases the computation time to reach a solution. As opposed to the crude coil model commonly used for EM-FE analysis, shown in Fig. 2(b), here an alternative representation is developed. According to Fig. 2(c), the winding is divided into a number of rectangular areas over its radial and tangential dimensions.

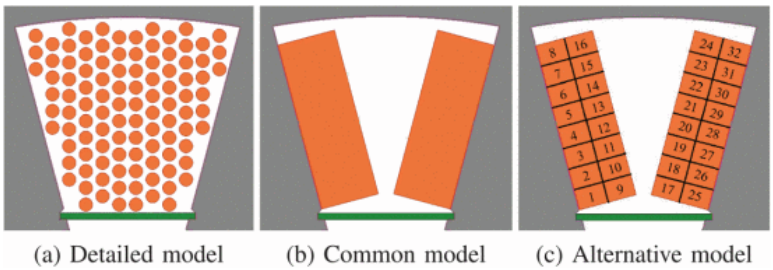

Fig. 2. Coil models for FE analysis of a typical electric machine.

The heights and the widths of the sections can be all equal or skewed to provide more details at the slot opening. In Fig. 2(c), 32 sections with equal heights and equal widths are defined. The number of sections should be selected so that a reasonable distribution of B samples are obtained within the slot. The radial and tangential components of the flux densities at the

middle of each rectangular section can then be extracted. The sampled B profiles are subsequently used to map the flux density at any point in the slot.

B. Extraction of B Field Profiles Inside the Slot

The value of B at the middle of each section can be obtained by any time-stepping magnetostatic FE analysis including the computationally efficient FEA (CE-FEA) method introduced in,[21] which exploits the electric symmetry in the stator windings of sinewave operated/energized PM motors. Using CE-FEA, the profile of the flux density waveforms over the full electrical cycle can be reconstructed by performing FEA over a window of 60 elec. deg.

Here, the CE-FEA method is used to extract the radial and tangential components of the sampled B profiles for the coil pieces shown in Fig. 2(c) for a typical machine under full-load motoring operation with counterclockwise rotation. The profiles for selected sections are shown in Figs. 3(a) through (d). It is interesting to note that the major component of the slot leakage flux is tangential. Furthermore, the decreasing trend of this slot leakage flux from top to bottom of the slot, and from left to right for the motoring operation, should be noted.

C. Determination of the Slot Fill Factor and the Associated Conductor Positions

The slot fill factor, s_f, is defined as follows:

$$s_f = \frac{A_{Cu}}{A_{slot}} = \frac{n_C \pi d^2}{4 A_{slot}} \quad (6)$$

where A_{Cu} is the copper area within the slot area, A_{slot}, and n_C is the number of conductors. In a large-scale design optimization problem, the slot dimensions and area vary between the design candidates. Accordingly, the maximum slot fill factor, $s_{f,max}$, and the location of the conductors vary between the design candidates and should be calculated for each individual design. Here, the $s_{f,max}$ is needed for the FEA to accurately account for the available Ampere Turn flowing through the alternate coil model described in the previous section. Furthermore, the conductor positions inside the slot are required for determining the impinging field on each strand in a post-FEA process using the B samples from FEA. This mapping process will be described in a later section.

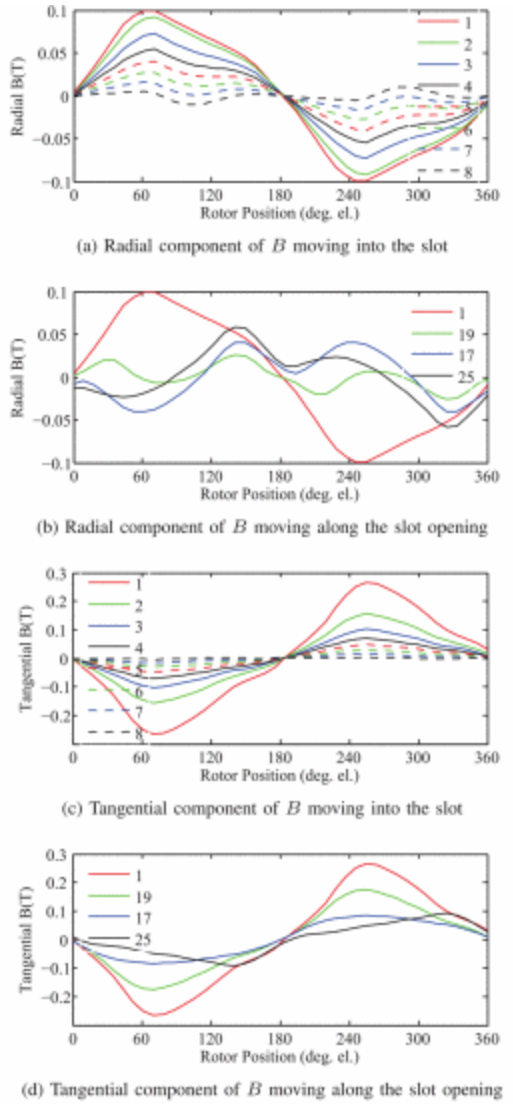

(a) Radial component of B moving into the slot

(b) Radial component of B moving along the slot opening

(c) Tangential component of B moving into the slot

(d) Tangential component of B moving along the slot opening

Fig. 3. Radial and tangential components of the field sections in fig. 2(c) for a typical motor.

The method that was implemented here for the calculation of $s_{f,max}$ and the associated positions of the conductors within the slot, which yields such $s_{f,max}$, relies on an optimization approach that is based on random perturbation of the slot geometry.[22] As can be seen in Fig. 4, a given slot geometry is randomly moved with respect to a grid of tightly packed circular conductors. The fill factor is then compared for various slot perturbations and strand arrangements to determine the $s_{f,}$ max and the associated locations of the strands.

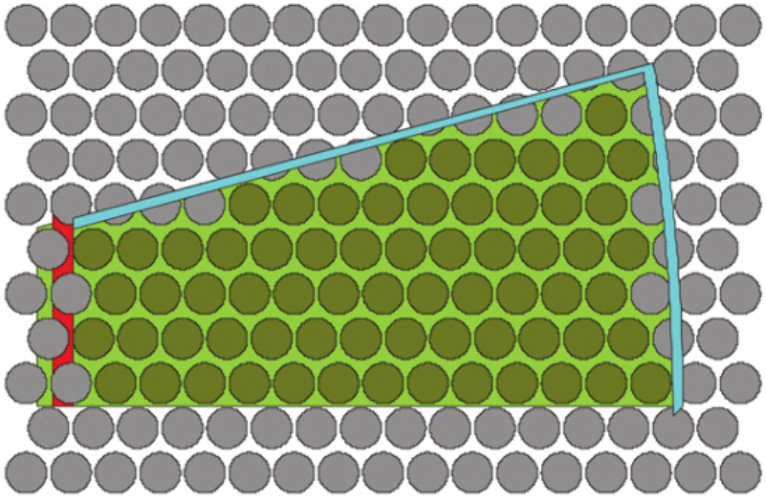

Fig. 4. Determination of $s_{f,max}$ and conductor positions by moving the slot geometry over a grid of conductors.

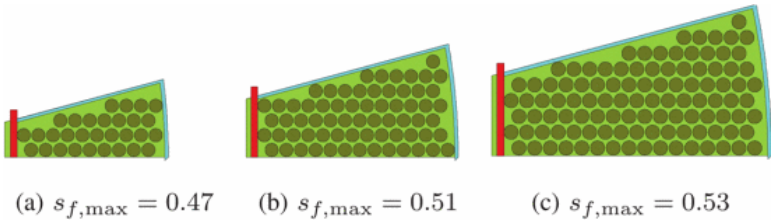

Fig. 5. Slot fill factor and strand positions for example slot geometries as the net slot area increases.

This method is used for the determination of $s_{f,max}$ in the example slot geometries shown in Figs. 5(a) through (c). As can be seen in this illustration, for a given conductor diameter, the achievable $s_{f,max}$ diminishes as the slot area decreases, which is successfully predicted by the method implemented here.

D. Mapping the Flux on Each Individual Strand

When the B profiles over the full fundamental cycle are obtained for each rectangular coil section, the radial and tangential components are separately used in a time harmonic analysis according to (1). Subsequently, for each harmonic, a Delaunay triangulation method is implemented in MATLAB for interpolating the samples scattered over the slot at the points where the center of each strand conductor is located. This process is illustrated in Fig. 6 for the reconstruction surfaces of the first harmonic of the B field throughout the slot area.

The order of harmonics that should be included is design dependent. When the field values throughout the slot area are determined, using the prior information of the strand positions, the impinging field on each strand can be mapped. In Fig. 7, the mapped values of the impinging B over each strand are shown for the fundamental and the third field harmonics. It can be seen once again that the magnitude of the slot leakage flux density monotonically increases for the strands that are closer to the air gap. The same trend exists for strands that are located towards the leading end of the rotor pole under motoring operation for CCW direction of rotation.

E. Estimation of Value and Distribution of Eddy Current Losses

Upon derivation of the impinging $|B|$ on each strand, depending on the conductor shape, the loss models given in (2)–(5) can be used for estimation of strand eddy current losses in the conductors at the strand level. The resultant loss values using such an analysis on a typical slot is shown in Figs. 8(a) through (f) for a wide range of loading levels.

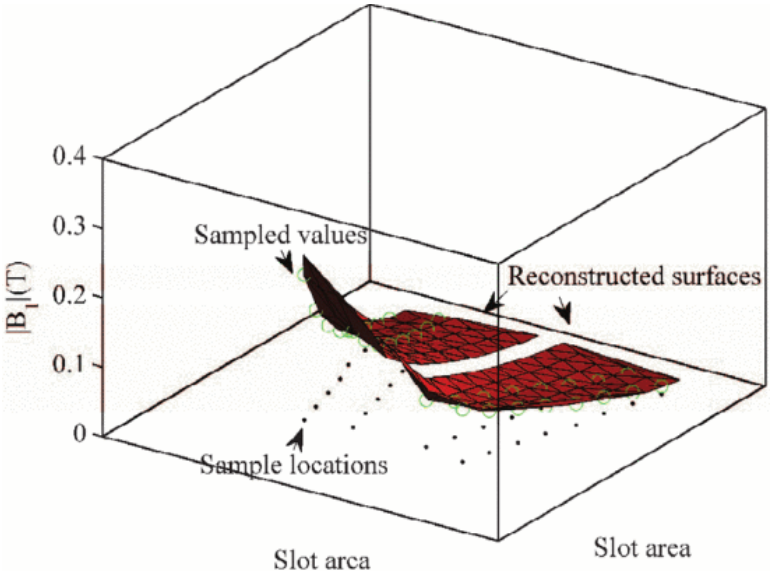

Fig. 6. Reconstruction of the field harmonics from the sample points using delaunay triangulation method.

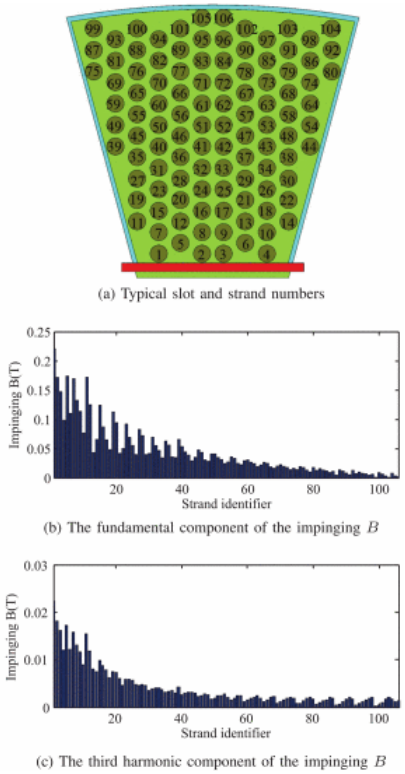

Fig. 7. Mapped flux on each individual strand.

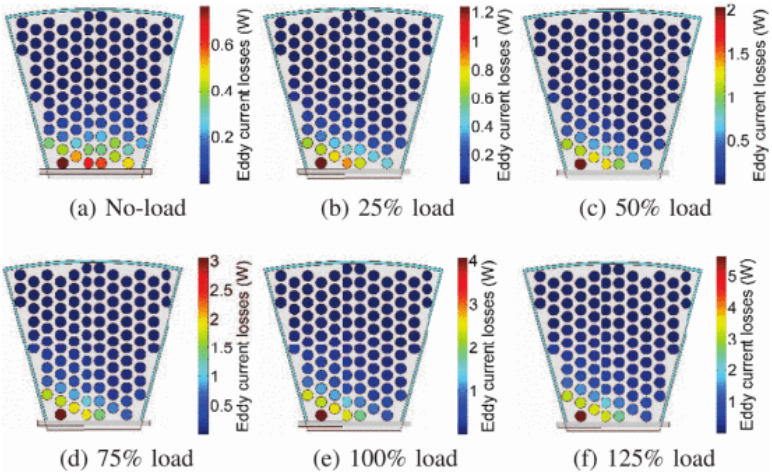

Fig. 8. Distribution of strand eddy current losses at different loading conditions. Note that the scales of the color-coded plots are different.

As can be seen in Fig. 8, using the developed method, in addition to the overall value of the eddy current losses, the distribution of such losses over each strand is obtained, which enables the incorporation of such losses into thermal analysis of the slot body.

SECTION IV.

Case-Study Analysis and Experimental Verification on 12-Slot 10-Pole Machines

The method developed here was used for the calculation of eddy current losses in a 12-slot 10-pole IPM machine with V-type magnet layouts as shown in Fig. 9(a). The all-teeth-wound stator winding consists of series coils each composed of 53 turns of AWG 12.5 wires, thus reducing to negligible levels the losses associated with circulating currents, which are essentially of a three-dimensional nature and cannot be accounted for by two-dimensional models.

The stator winding losses including the strand eddy current losses are calculated by the developed method and the results are compared with those obtained from a time-stepping FEA with detailed coil modeling as shown in Fig. 9(b).

The strand eddy current losses are calculated over a wide range of motor loading conditions under MTPA control for three different speeds at a winding temperature of 100°C. The results obtained from the developed method and those from the time harmonic FEA with detailed coil modeling are compared in Figs. 10(a)–(c). The required computation time is less than 80 seconds using the proposed method as opposed to 3370 seconds using the detailed FEA.

The estimation error of the proposed method when compared to the detailed TS-FE model is shown in Fig. 11 for several speeds and over a wide range of loading. The error is within a reasonable range given the computational efficiency of the proposed method.

The variation of the ac to dc loss ratio, P_{ac}/P_{dc}, due to the armature reaction under different loading levels is shown in Fig. 13. As can be seen in Figs. 13(a) through (c), strand eddy current losses constitute a larger contribution to the overall losses, $P_{ac} = P_{dc} + P_e$, under light load levels. The rate of increase of eddy current losses with respect to loading, which is mainly due to the elevated saturation level of the ferrous core and therefore increased leakage and fringing of flux into the slot area, is less than the rate of increase of dc copper losses P_{dc}, which is directly proportional to the current squared. This is especially true at lower frequencies as can be seen in Fig. 12. However, the eddy current losses are constantly present even at no-load conditions due to the presence of the time-varying field in the slots.

2016 IEEE Energy Conversion Congress and Exposition (ECCE), (2016). DOI.

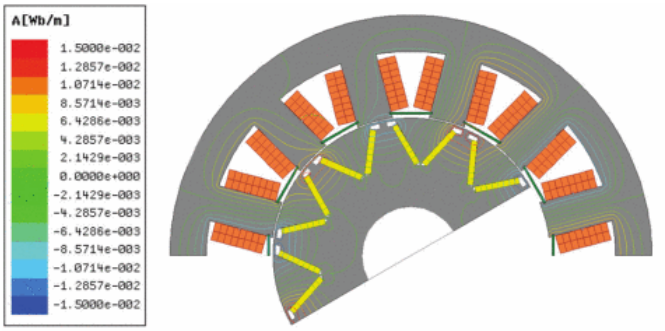

(a) CE-FEA with flux mapping

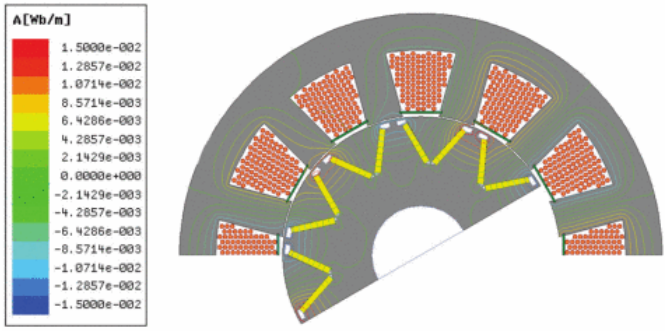

(b) FEA with detailed coil modeling

Fig. 9. Case-study investigation of a 10 hp generic industrial 12-slot 10-pole machine.

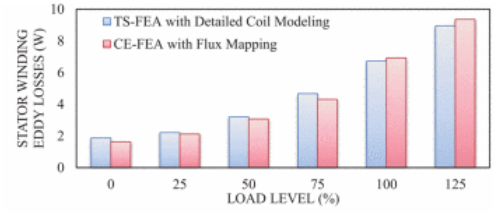

(a) 150 Hz

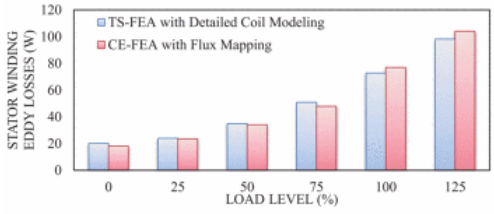

(b) 500 Hz

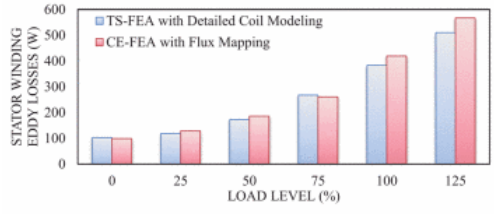

(c) 1200 Hz

Fig. 10. Comparison of the accuracy of the loss calculation method over a wide range of frequencies and loading conditions.

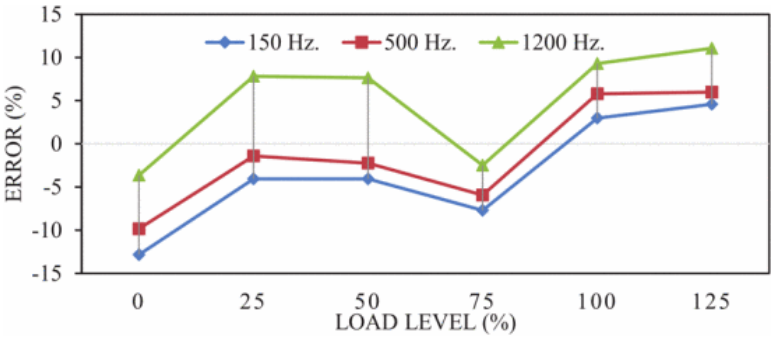

Fig. 11. Estimation error of the computationally efficient method of calculation of strand eddy current losses compared to the full-fledged time harmonic analysis with detailed coil modeling.

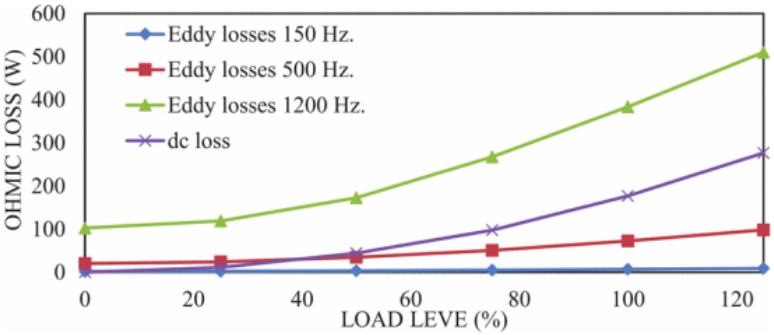

Fig. 12. Variation of dc ohmic losses and strand eddy current losses with respect to loading level.

The ratio of R_{ac}/R_{dc}, which is commonly used in the literature, is by definition not exposed to such large variations, and thus does not reflect them. Therefore, if the ratio of R_{ac}/R_{dc} is to be used as a figure of merit for comparison of ac losses between different design solutions, it should be derived and formulated under various loading conditions.[23]

Here, for experimental demonstration of variation of R_{ac}/R_{dc} with respect to frequency, and under one particular loading condition, the loss derivation method introduced in[19] is used. According to this method, several R_{ac}/R_{dc} input data points are experimentally derived taking into account the end windings and bundle-level proximity effects, which cannot be accounted for by two-dimensional methods such as the one presented in this paper. Accordingly, for the stator assembly of a 12-slot 10-pole IPM machine with mush wound multi-stranded double layer concentrated winding shown in Fig. 14(a), the measured ac winding losses are obtained at different frequencies using the setup shown in Fig. 14(b). The resultant R_{ac}/R_{dc}, which was

obtained at 23 °C, is plotted in Fig. 15. The final winding power loss, including the effects of temperature can be estimated using (7) below:[19]

$$P_{ac|T} = P_{dc|T_0}(1 + \alpha(T - T_0)) + P_{dc|T_0}\frac{\frac{R_{ac}}{R_{dc}}|_{T_0} - 1}{(1 + \alpha(T - T_0))^{\beta}} \quad (7)$$

where $P_{dc|T_0} = 3R_{dc}|_{T_0} I_{ph,rms}^2$, α is the temperature coefficient of resistivity for copper conductors $\alpha = 3.93 \times 10^3 K^1$, and β<1 is an introduced factor that can be found by curve fitting (7) into the ac copper loss data for temperature T.[19] However, as shown through the analysis of the ac losses in the previous section, an additional curve fitting is required to account for comprehensive loss estimation at different loading conditions. This additional curve fitting is beyond the scope of this paper and will be investigated in a future work.

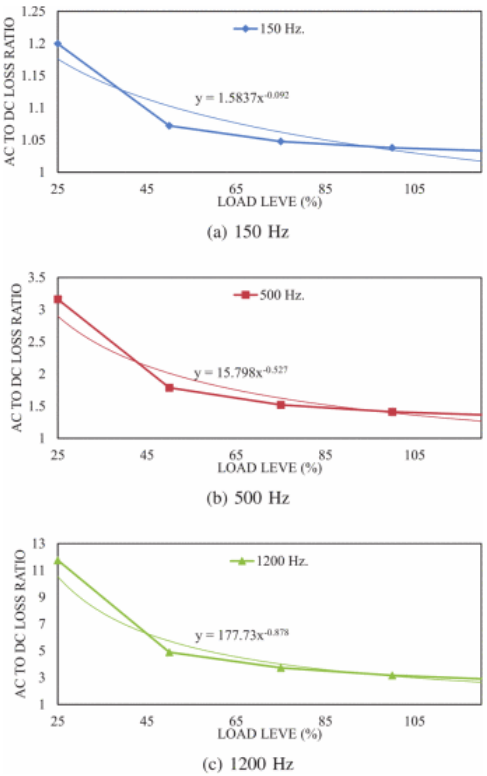

Fig. 13. Ratio of ac to dc losses over a wide range of loading conditions.

As mentioned previously, the presented ac loss calculation method yields both the overall eddy current ac losses due to the slot leakage and fringing flux, and also the distribution of such

losses within the slot. The latter can be used for thermal analysis of the design candidates in a coupled electromagnetic-thermal optimization process.[2,3]

Here, to illustrate how the inclusion of the strand eddy current losses influences the temperature distribution within the slots, the thermal performance of the case study motor in Fig. 9 is investigated. The thermal analysis is carried out in Motor-CAD, Fig. 16(b), which relies on fast lumped parameter thermal models suitable for coupled thermal-electromagnetic optimizations as presented in.[2] For this purpose, a typical liquid-based cooling system with stator water jackets as shown in Fig. 16(a) is considered. The coolant is water with a flow rate of 10 lit/min and an inlet temperature of 40°C.

(a) Winding process of the randomly wound 12-slot 10-pole machine

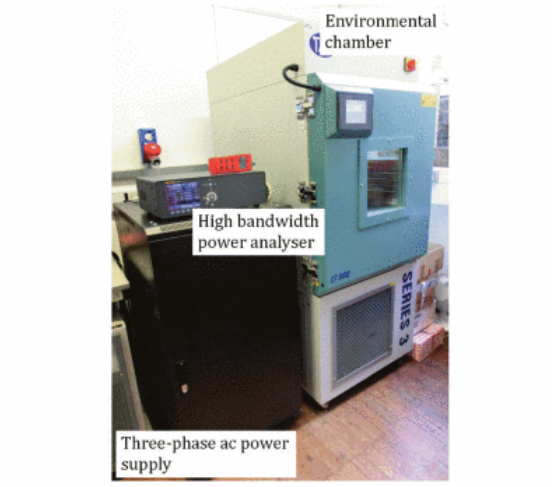

(b) Experimental setup used for measurement of ac winding losses

Fig. 14. Setup for demonstration of variation of R_{ac}/R_{dc}.

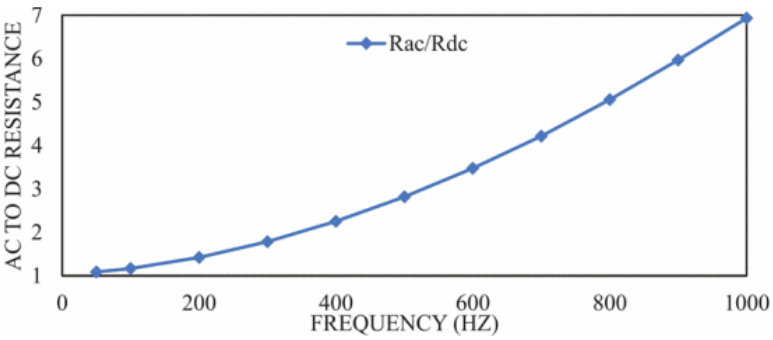

Fig. 15. Measured R_{ac}/R_{dc} ratio versus excitation frequency at a winding temperature of 23 ° C.

Two scenarios are considered for this thermal analysis based on whether the strand eddy current losses are included, or only the dc ohmic losses are taken into account. The resultant average and maximum temperatures obtained for full load operation under three different speeds, namely, 1,800 r/min, 6,000 r/min, and 14,000 r/min are listed in Tables I and II. The large discrepancies in the temperatures obtained from the two scenarios based on whether or not the strand eddy current losses are included in the thermal analysis, especially as the speed, and thus the frequency of operation, increases should be noted.

Table I Winding temperatures based on DC ohmic losses only

Speed	Max. Temperature	Ave. Temperature
1,800 r/min	75.8 °C	47.9 °C
6,000 r/min	84.0 °C	59.4 °C
14,000 r/min	129.7 °C	86.0 °C

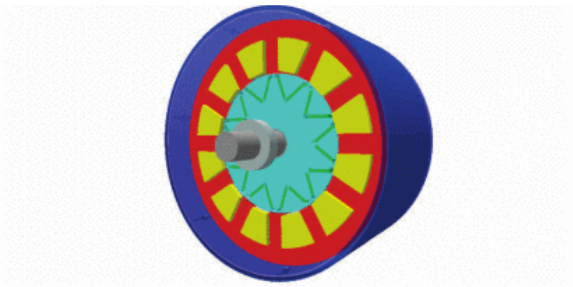

(a) Liquid-based cooling system with stator water jackets developed in Motor-CAD

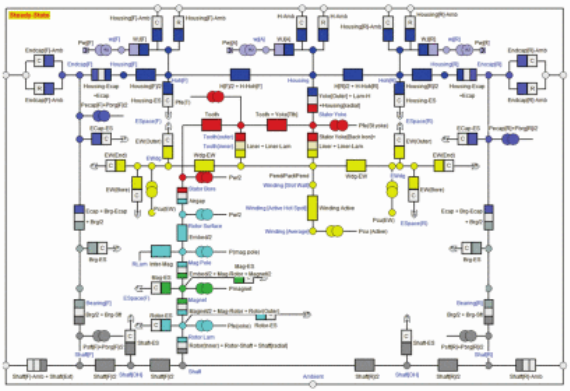

(b) Lumped parameter thermal model

Fig. 16. Thermal performance analysis for the case study motor in fig. 9.

Table II Winding temperatures including stator winding strand eddy current losses

Speed	Max. Temperature	Ave. Temperature
1,800 r/min	77.4 °C	65.3 °C
6,000 r/min	101.9 °C	85.2 °C
14,000 r/min	200.8 °C	162.4 °C

SECTION V.

Conclusions

A method was developed for the calculation of strand eddy current losses in the stator windings of electric machines that (a) is finite-element based to take into account the complex geometry of the machine and the effects of saturation, (b) is computationally efficient and suitable for integration into large-scale design optimization algorithms, (c) is applicable to any variety of machines with different combinations of stator slots and rotor pole structures, (d) estimates the maximum SF factor for each design candidate based on winding specs and slot geometry, (e) estimates the value of eddy current losses due to slot leakage and fringing flux effects under any loading conditions, i.e. various torque and speed operating points, and (f)

estimates the distribution of copper losses including the eddy current losses in the slots for rigorous thermal analysis of the stator windings.

The developed loss calculation method was implemented on a FSCW 12-slot 10-pole IPM machine with relatively large slot openings. The results over a wide range of loading conditions and operating frequencies were in good agreement with those obtained from a time harmonic FEA with detailed coil modeling. Meanwhile the required computation time was significantly reduced using the presented method. The distribution of the losses in this case study machine were used for a subsequent thermal performance analysis to underscore the importance of including strand eddy losses as a major loss component in high speed machines, even if the stator winding conductors are stranded and transposed.

Using the developed loss calculation method, it was also shown that the variations of P_{ac}/P_{dc} loss ratio with reference to the machine loading levels are not reflected in the common figure of merit represented by R_{ac}/R_{dc} resistance ratio. Thus if the R_{ac}/R_{dc} ratio is to be used, additional treatment will be required to include the loading effects.

ACKNOWLEDGMENTS

The authors are thankful to SEMPEED Consortium, and MWERC Consortium for partial financial support. The authors also gratefully acknowledge the software support of Motor Design Ltd., and ANSYS Inc.

References

[1]E. Snelling, Soft ferrites: properties and applications, Butterworths, 1988.

[2]Y. Wang, D. Ionel, D. Staton, "Ultrafast Steady-State Multiphysics Model for PM and Synchronous Reluctance Machines", *Industry Applications IEEE Transactions on*, vol. 51, no. 5, pp. 3639-3646, 2015.

[3]W. Jiang, T. Jahns, "Coupled electromagnetic-thermal analysis of electric machines including transient operation based on finite element techniques", *Energy Conversion Congress and Exposition (ECCE) 2013 IEEE*, pp. 4356-4363, 2013.

[4]M. Popescu, D. Dorrell, "Proximity Losses in the Windings of High Speed Brushless Permanent Magnet AC Motors With Single Tooth Windings and Parallel Paths", *Magnetics IEEE Transactions on*, vol. 49, no. 7, pp. 3913-3916, 2013.

[5]L. Wu, Z. Zhu, D. Staton, M. Popescu, D. Hawkins, "Analytical Model of Eddy Current Loss in Windings of Permanent-Magnet Machines Accounting for Load", *Magnetics IEEE Transactions on*, vol. 48, no. 7, pp. 2138-2151, 2012.

[6]P. Reddy, T. Jahns, T. Bohn, "Modeling and analysis of proximity losses in high-speed surface permanent magnet machines with concentrated windings", *Energy Conversion Congress and Exposition (ECCE) 2010 IEEE*, pp. 996-1003, 2010.

[7]W. Zhang, T. Jahns, "Analytical 2-D slot model for predicting AC losses in bar-wound machine windings due to armature reaction", *Transportation Electrification Conference and Expo (ITEC) 2014 IEEE*, pp. 1-6, 2014.

[8]A. Thomas, Z. Zhu, G. Jewell, "Proximity Loss Study In High Speed Flux-Switching Permanent Magnet Machine", *Magnetics IEEE Transactions on*, vol. 45, no. 10, pp. 4748-4751, 2009.

[9]P. Reddy, Z. Zhu, S.-H. Han, T. Jahns, "Strand-level proximity losses in PM machines designed for high-speed operation", *Electrical Machines 2008. ICEM 2008. 18th InternationalConference on*, pp. 1-6, 2008.

[10]Y. Amara, P. Reghem, G. Barakat, "Analytical Prediction of Eddy-Current Loss in Armature Windings of Permanent Magnet Brushless AC Machines", *Magnetics IEEE Transactions on*, vol. 46, no. 8, pp. 3481-3484, 2010.

[11]A. Bellara, H. Bali, R. Belfkira, Y. Amara, G. Barakat, "Analytical Prediction of Open-Circuit Eddy-Current Loss in Series Double Excitation Synchronous Machines", *Magnetics IEEE Transactions on*, vol. 47, no. 9, pp. 2261-2268, 2011.

[12]L. Wu, Z. Zhu, "Analytical investigation of open-circuit eddy current loss in windings of PM machines", *Electrical Machines (ICEM) 2012 XXth InternationalConference on*, pp. 2759-2765, 2012.

[13]N. A. Demerdash, H. Hamilton, "Effect of Rotor Asymmetry on Field Forms and Eddy Current Losses in Stator Conductors Due to Radial Flux", *Power Apparatus and Systems IEEE Transactions on*, vol. PAS-91, no. 5, pp. 1999-2010, 1972.

[14]S. Iwasaki, R. Deodhar, Y. Liu, A. Pride, Z. Zhu, J. Brem-ner, "Influence of PWM on the Proximity Loss in Permanent-Magnet Brushless AC Machines", *Industry Applications IEEE Transactions on*, vol. 45, no. 4, pp. 1359-1367, 2009.

[15]A. Arkadan, R. Vyas, J. Vaidya, M. Shah, "Effect of toothless stator design and core and stator conductors eddy current losses in permanent magnet generators", *Energy Conversion IEEE Transactions on*, vol. 7, no. 1, pp. 231-237, 1992.

[16]R.-J. Wang, M. Kamper, "Calculation of eddy current loss in axial field permanent-magnet machine with coreless stator", *Energy Conversion IEEE Transactions on*, vol. 19, no. 3, pp. 532-538, 2004.

[17]P. Mellor, R. Wrobel, D. Salt, A. Griffo, "Experimental and analytical determination of proximity losses in a high-speed PM machine", *Energy Conversion Congress and Exposition (ECCE) 2013 IEEE*, pp. 3504-3511, 2013.

[18]R. Wrobel, J. Goss, A. Mlot, P. Mellor, "Design Considerations of a Brushless Open-Slot Radial-Flux PM Hub Motor", *Industry Applications IEEE Transactions on*, vol. 50, no. 3, pp. 1757-1767, 2014.

[19]R. Wrobel, D. Salt, A. Griffo, N. Simpson, P. Mellor, "Derivation and Scaling of AC Copper Loss in Thermal Modeling of Electrical Machines", *Industrial Electronics IEEE Transactions on*, vol. 61, no. 8, pp. 4412-4420, 2014.

[20]G. Carter, The electromagnetic field in its engineering aspects ser. Electrical engineering series, American Elsevier Pub. Co., 1967.

[21]P. Zhang, G. Sizov, J. He, D. Ionel, N. Demerdash, "Calcu-lation of Magnet Losses in Concentrated-Winding Permanent-Magnet Synchronous Machines Using a Computationally Efficient Finite-Element Method", *Industry Applications IEEE Transactions on*, vol. 49, no. 6, pp. 2524-2532, 2013.

[22]G. Y. Sizov, "Design synthesis and optimization of permanent magnet synchronous machines based on computationally-efficient finite element analysis" in , Marquette University, 2013.

[23]R. Wrobel, A. Mlot, P. H. Mellor, "Contribution of End-Winding Proximity Losses to Temperature Variation in Electromagnetic Devices", *IEEE Transactions on Industrial Electronics*, vol. 59, no. 2, pp. 848-857, 2012.